THE JOURNAL OF PHYSICAL CHEMISTRY B

Article

pubs.acs.org/JPCB

Determination of ^{15}N Chemical Shift Anisotropy from a Membrane-Bound Protein by NMR Spectroscopy

Manoj Kumar Pandey,[†] Subramanian Vivekanandan,[†] Shivani Ahuja,[†] Kumar Pichumani,[‡] Sang-Choul Im,[§] Lucy Waskell,[§] and Ayyalusamy Ramamoorthy*,[†]

[†]Biophysics and Department of Chemistry, University of Michigan, Ann Arbor, Michigan 48109-1055, United States

[‡]Advanced Imaging Research Center, University of Texas Southwestern Medical Center, 2201 Inwood Road, Dallas, Texas 75390-8568, United States

[§]Department of Anesthesiology, University of Michigan and VA Medical Center, Ann Arbor, Michigan 48105, United States

Supporting Information

ABSTRACT: Chemical shift anisotropy (CSA) tensors are essential in the structural and dynamic studies of proteins using NMR spectroscopy. Results from relaxation studies in biomolecular solution and solid-state NMR experiments on aligned samples are routinely interpreted using well-characterized CSA tensors determined from model compounds. Since CSA tensors, particularly the ^{15}N CSA, highly depend on a number of parameters including secondary structure, electrostatic interaction, and the amino acid sequence, there is a need for accurately determined CSA tensors from proteins. In this study, we report the backbone amide-^{15}N CSA tensors for a 16.7-kDa membrane-bound and paramagnetic-heme containing protein, rabbit Cytochrome b_5 (cytb$_5$), determined using the ^{15}N CSA/^{15}N−^{1}H dipolar transverse cross-correlation rates. The mean values of ^{15}N CSA determined for residues in helical, sheet, and turn regions are −187.9, −166.0, and −161.1 ppm, respectively, with an overall average value of −171.7 ppm. While the average CSA value determined from this study is in good agreement with previous solution NMR experiments on small globular proteins, the CSA value determined for residues in helical conformation is slightly larger, which may be attributed to the paramagnetic effect from Fe(III) of the heme unit in cytb$_5$. However, like in previous solution NMR studies, the CSA values reported in this study are larger than the values measured from solid-state NMR experiments. We believe that the CSA parameters reported in this study will be useful in determining the structure, dynamics, and orientation of proteins, including membrane proteins, using NMR spectroscopy.

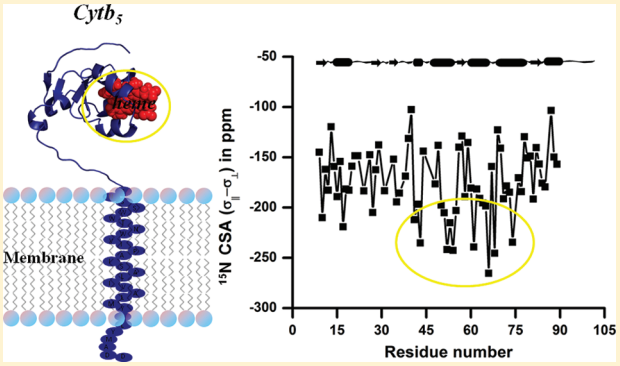

INTRODUCTION

Solving high-resolution structures and characterization of dynamics of biomolecules has become one of the most important goals of modern structural biology. Both solution and solid-state NMR spectroscopic techniques are increasingly used to study the structure and dynamics of proteins. In these NMR studies, chemical shift anisotropy (CSA) tensors play a vital role in providing valuable information about the local structure and motions surrounding a nucleus. In solids, molecular motions are restricted as a result anisotropic interactions such as CSA, and dipolar interactions are present in totality. CSA tensors from solids can be determined using various methods: static powder patterns,[1−4] two-dimensional (2D) separated-local-field (SLF) experiments,[5,6] magic angle spinning (MAS) spectra,[7−12] recoupling techniques[13,14] and single-crystal studies.[15−17] In addition, quantum chemical calculations have also contributed significantly toward computing and understanding the variation of CSA tensors.[18−25] Solid-state NMR spectroscopy is also commonly used for CSA measurements from samples that are site specifically labeled with an isotope (such as ^{15}N or ^{13}C). However, this technique is less practical for large proteins that are isotopically labeled at multiple sites due to difficulties associated with severe spectral overlap. On the other hand, this problem can be overcome by studying these proteins in solution. The rapid tumbling of the molecules in solution results in a faster change of molecular orientations than the magnitude of anisotropic interactions leading to well-resolved narrow lines at the isotropic chemical shift values. Hence, information about individual components of the CSA tensor cannot be determined from the peak positions. However, recent studies have shown that the CSA tensor elements for globular proteins can be determined in solution from nuclear spin relaxation measurements where CSA contributes to relaxation through a cross-correlation relaxation mechanism with a dipolar coupling tensor.[26−33]

Received: March 7, 2012
Published: May 23, 2012

   dx.doi.org/10.1021/jp3049229 | J. Phys. Chem. B 2012, 116, 7181−7189

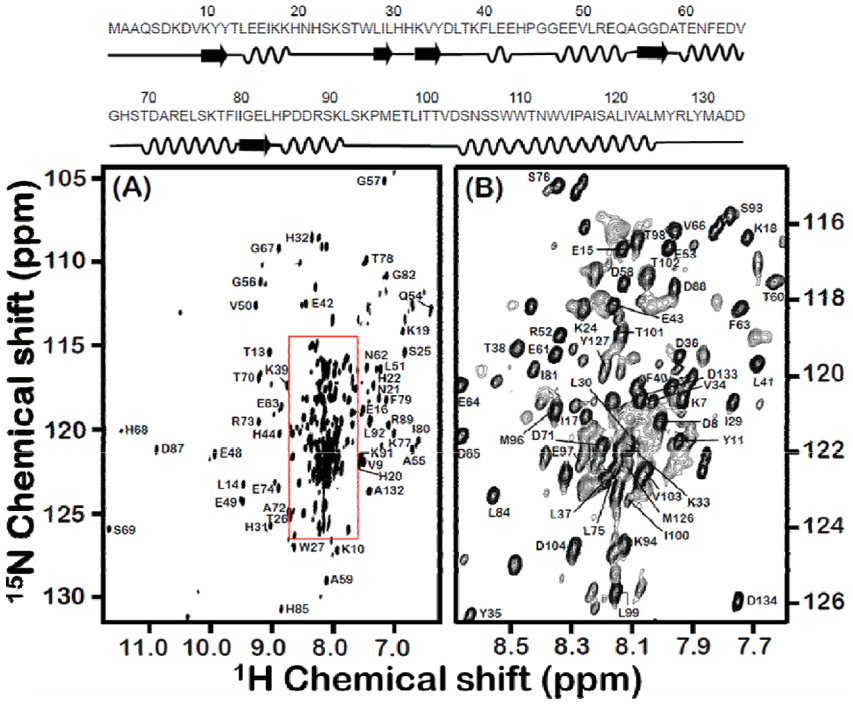

Figure 1. Backbone amide resonance assignment for the 16.7-kDa rabbit cytb$_5$ incorporated in DPC micelles. A full 2D ^{15}N−^{1}H TROSY-HSQC spectrum of U−^{13}C, ^{15}N, ^{2}H-labeled full-length cytb$_5$ in DPC micelles along with resonance assignments is shown in panel A, while panel B represents expanded region of the box shown in panel A. The amino acid sequence with its secondary structure is shown at the top.

There is a growing interest in determining amide-^{15}N CSA tensors associated with the backbone of a protein. Well-characterized amide-^{15}N CSA tensors are essential to determine the structure and local dynamics, and to distinguish the residues undergoing conformational exchange. Structural dependence of ^{1}H and ^{13}C chemical shifts are well studied by experimental as well as computational approaches both in solids and solutions.[10,14,34−40] ^{15}N CSA, on the other hand, is relatively less known, as it is influenced by many factors such as torsion angles, hydrogen bonding interactions (both intra and inter residue), intraresidue angles, the chemical nature of a side chain, electrostatic interactions, and solvent interactions.[23,41−47] Many attempts have also been made toward theoretical determination of ^{15}N CSA using quantum chemical methods by several groups in the recent past.[19,43,48−55] Experimentally, the most widely used method to obtain ^{15}N CSA values from proteins in solution is by measuring the cross-correlation rate arising due to the interference between ^{15}N CSA and ^{15}N−^{1}H dipolar coupling tensors that lead to differential line broadening of the ^{15}N doublet components in ^{1}H-coupled ^{15}N−^{1}H HSQC (heteronuclear single quantum coherence) spectra.[28−31,56−59] Long-range cross-correlation rate measurements have also been reported for ^{13}CO CSA and weak dipolar interaction between the same carbonyl and neighboring amide proton.[33,60] A recent study makes use of different motional models to describe local motions for the determination of CSA tensor components in human ubiquitin and shows that the measured CSA values are weakly dependent on the choice of model used for the study.[26] Hall and Fushman obtained similar results for backbone amide-^{15}N CSA values in protein G by applying a combination of relaxation and CSA/dipolar cross-correlation measurements at five different magnetic fields using various model independent approaches.[61] Damberg et al. have shown limited variations in the magnitude and orientation of site-specific backbone amide-^{15}N CSA in ubiquitin measured at four different magnetic field strengths.[62] In another study, site-specific backbone amide-^{15}N CSA tensors for the well-ordered B3 domain of globular binding protein were determined from residual chemical shift anisotropy (RCSA) measurements.[63] In the present study, we measure the backbone amide-^{15}N CSA in combination with transverse CSA/dipolar cross-correlation rates for a membrane protein Cytochrome b_5 (cytb$_5$) using a ^{1}H coupled ^{15}N−^{1}H HSQC type spectra by comparing the observed difference in line widths of the ^{15}N doublet components using a model independent method developed by Fushman et al.[29] Cytb$_5$ is a 16.7-kDa (134 amino acid residues) electron transfer protein present in eukaryotic organisms. It contains a structured water-soluble domain with a paramagnetic heme unit, a transmembrane helical domain, and an unstructured about 14-residues long linker region that connects the transmembrane and soluble domains of cytb$_5$.[64−66] Since this membrane-bound protein is rich in different secondary structural elements and domains exhibiting a range of dynamics and a paramagnetic center, it makes an excellent model system to study the variations in the amide-^{15}N CSA tensors with structure and dynamics. Our results indeed provide an explanation for the variation of experimentally measured amide-^{15}N CSA tensors that will be useful in the structural studies of water-soluble as well as membrane-associated proteins.

EXPERIMENTAL SECTION

A membrane-bound cytb$_5$ was expressed in *Escherichia coli* and purified as explained elsewhere.[67] The ^{15}N−^{1}H HSQC type proton coupled IPAP (in-phase/antiphase) experiments[56] for transverse cross-correlation rate measurements were performed on a 900 MHz Bruker Avance NMR spectrometer using a cryo probe. A 5 mm Shigemi tube containing 0.5 mL of a 0.3 mM

dx.doi.org/10.1021/jp3049229 | J. Phys. Chem. B 2012, 116, 7181−7189

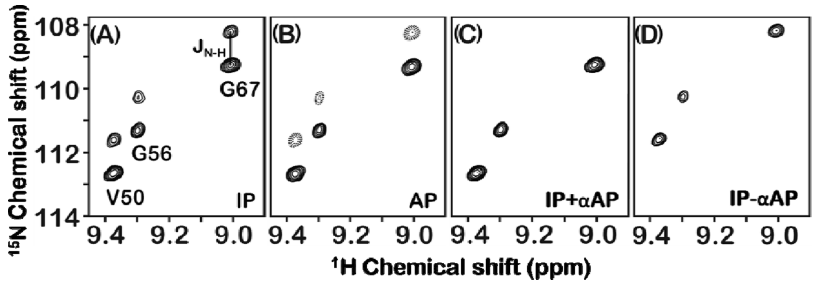

Figure 2. Representative regions of ^{1}H coupled 2D ^{15}N−^{1}H HSQC spectra. The plot is extracted from a small region of the 2D ^{15}N−^{1}H HSQC spectrum of a uniformly-^{15}N, ^{13}C and ^{2}H-labeled cytb$_5$ incorporated in DPC micelles. The spectra were recorded using a relaxation delay of 10.64 ms from a 900 MHz NMR spectrometer. Protons were not decoupled during the t_1 period of the pulse sequence and therefore the transverse magnetization of ^{15}N nuclei was allowed to evolve under ^{15}N chemical shift and ^{15}N−^{1}H scalar couplings. Panels A, B, C, and D represent the IP ^{15}N−^{1}H doublets, the AP ^{15}N−^{1}H doublets, the simplified sum (IP+αAP) and the difference (IP−αAP) spectra, respectively.

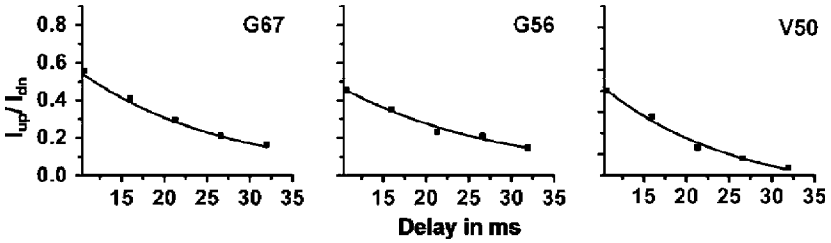

Figure 3. Determination of transverse cross-correlation rates, η_{xy}. The plots represent monoexponential decay curves for the measurement of transverse cross-correlation rates (η_{xy}) from the ratio of the upfield and the downfield peak intensities (I_{up}/I_{dn}) for residues G67, G56, and V50 against the delay time (Δ). The corresponding values of η_{xy} for these residues are 12.43 ± 0.50 s^{-1}, 13.29 ± 1.10 s^{-1}, and 16.05 ± 1.12 s^{-1}, respectively.

uniformly labeled ^{13}C, ^{2}H, ^{15}N cytb$_5$ sample incorporated in 45 mM perdeuterated dodecylphosphocholine (DPC) in 100 mM potassium phosphate (KPi) buffer at pH 7.4, containing 5% glycerol and 35% D_2O at 25 °C was used in all NMR experiments. The relaxation delay (Δ) values were set to 10.64, 15.96, 21.28, 26.60, and 31.92 ms, and the IPAP spectra were collected in an interleaved manner as pseudo-three-dimesional (3D) experiments where the first 2D-plane corresponds to in-phase (IP) and the second plane to antiphase (AP) spectra. The same number of scans was used for the IP and AP experiments for a given delay, while it was varied from 24 for the smallest to 96 for the largest delay to compensate for the loss of signal due to a large delay Δ in the IPAP pulse sequence. Experimental data processing and the subsequent addition/subtraction of IP and AP spectra were performed using NMRpipe,[68] while resonance peak assignments for cytb$_5$ were done using Sparky.[69]

RESULTS AND DISCUSSION

The amino acid sequence of a 16.7-kDa rabbit cytb$_5$ and a 2D ^{15}N−^{1}H TROSY-HSQC[70] spectrum of U−^{13}C, ^{15}N, ^{2}H-labeled full-length cytb$_5$ incorporated in perdeuterated DPC detergent micelles at 25 °C are given in Figure 1. The amide NH resonances from the soluble domain (6−91 residues) and the linker region (92−104 residues) are well resolved as seen in Figure 1. Resonances from the N-terminal (1−5) and transmembrane region of the protein (105−125 residues) were not observed due to their fast spin−spin relaxation that leads to broadening of spectral lines. The structure and orientation of the transmembrane domain was characterized using the 2D HIMSELF (heteronuclear isotropic mixing leading to spin exchange via the local field) sequence[71] based on the PIWIMz (polarization inversion by windowless isotropic mixing) pulse scheme[72] solid-state NMR experiment, on a full-length cytb$_5$ incorporated in aligned DMPC/DHPC bicelles. Details on the resonance assignment and the 3D structure of cytb$_5$ will be reported elsewhere. In this study, we report experimentally measured backbone amide-^{15}N CSA tensors of 84 residues from cytb$_5$ incorporated in DPC micelles. The backbone amide-^{15}N CSA tensors for the remaining residues could not be measured due to overlapping resonances.

Backbone Amide-^{15}N CSA/Dipolar Transverse Cross-Correlation Rate Measurement. To determine backbone amide-^{15}N CSA, we measured ^{15}N CSA/dipolar transverse cross-correlation rates for various residues of cytb$_5$ by following the method as described by Hall and Fushman.[56] The transverse cross-correlation rates were measured by implementing the IPAP method[73] wherein two spectra that are representatives of the IP and the AP ^{15}N doublet components were recorded as part of a single experiment. The transverse cross-correlation rate measurement depends on the ratio of the signal intensities of the difference (upfield) and the sum (downfield) spectra, which decays monoexponentially with increase in relaxation delays. A small region of the ^{1}H coupled ^{15}N−^{1}H HSQC (IPAP) spectrum with resolved IP and AP ^{15}N spin doublet components are shown in Figure 2A and 2B, respectively. The upfield ($I_{up,2I_yS_z+I_y}$) and the downfield ($I_{dn,2I_yS_z-I_y}$) components of the IP and AP doublets were subsequently added and subtracted leading to simplified sum (IP+αAP) and difference (IP−αAP) spectra (Figure 2C and 2D, respectively). A scaling factor α = 1.2 was applied to the AP spectrum before its addition or subtraction to the IP spectrum to compensate for the signal losses and to obtain a complete removal of unwanted signals.

The intensity of peaks from the sum (IP+αAP) and the difference (IP−αAP) HSQC spectra was measured using

dx.doi.org/10.1021/jp3049229 | J. Phys. Chem. B 2012, 116, 7181−7189

Sparky. The ratio of intensities of the upfield and the downfield peaks for various residues of cytb$_5$ was then calculated and plotted against the delay time used in the experiment; representative plots for residues G67, G56, and V50 of cytb$_5$ are shown in Figure 3. The ^{15}N transverse cross-correlation rates (η_{xy}) were measured by fitting the monoexponential decay curves obtained from the ratio of the upfield and the downfield peak intensities using $I_{up,2I_yS_z+I_y}/I_{dn,2I_yS_z-I_y} = Ce^{-4\eta_{xy}\Delta}$; where C is the ratio of signal decays (or t_1-dependent functions) associated with the upfield and the downfield intensities, Δ is the relaxation delay which was taken as multiples of $1/(2J_{N-H})$, and J_{N-H} represents the one bond scalar ^{15}N−^{1}H coupling.

The backbone amide-^{15}N transverse cross-correlation rates (η_{xy}) determined from the best-fitting monoexponential decay curves for various residues of cytb$_5$ are given in Table S1 (see the Supporting Information) and are plotted in Figure 4. As

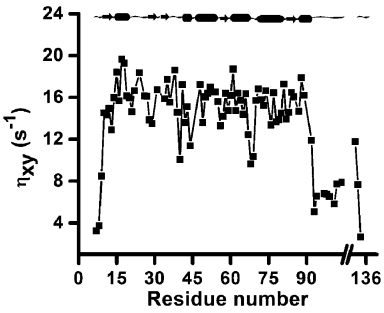

Figure 4. Backbone amide-^{15}N transverse cross-correlation rates, η_{xy}, for residues in a membrane-bound cytb$_5$. Backbone amide-^{15}N transverse cross-correlation rates as obtained from monoexponential decay curves are plotted against amino acid residue number of cytb$_5$. A break on the horizontal axis represents the transmembrane region of the protein that could not be observed in solution state NMR due to its fast spin−spin relaxation.

expected and also evident from Figure 4, the values of backbone amide-^{15}N transverse cross-correlation rates fall rapidly for residues in the N-terminus (residues 7−9), the C-terminus (residues 132−134), and the linker-region (residues 92−104) of cytb$_5$, which suggests a highly dynamic and flexible nature of the protein in these regions as compared to the structured regions.

Distribution of Backbone Amide-^{15}N Transverse Cross-Correlation Rates in Different Regions of cytb$_5$. The backbone amide-^{15}N transverse cross-correlation rates (η_{xy}) are receptive to internal and overall motions of the protein,[30,74] therefore structured elements such as α-helices, β-sheets, and turns may undergo differential dynamics in their 3D arrangement. Figure 5 shows a distribution of cross-correlation rates across α-helices, β-sheets, turns, and the loop-regions that include termini along with the linker-region across the amino acid sequence. It is evident from Figure 5 that there is hardly any difference between the mean values of backbone amide-^{15}N transverse cross-correlation rates for residues in α-helix (16.08 s^{-1}), β-sheet (15.05 s^{-1}), and turn (14.54 s^{-1}) regions. On the other hand, the mean value of the cross-correlation rate for residues in the termini and linker region is 6.83 s^{-1}. It should also be noted that the span of ^{15}N transverse cross-correlation rate values for α-helix and β-sheet residues is smaller than that for the turn and loop-region residues. This narrow distribution of cross-correlation rate suggests a uniform characteristic of the ^{15}N transverse cross-correlated relaxation rates in amide

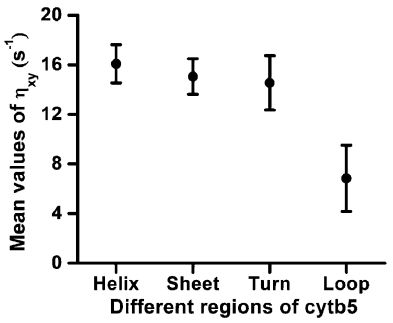

Figure 5. Distribution of backbone amide-^{15}N transverse cross-correlation rates in different regions of a membrane-bound cytb$_5$. The mean values of transverse cross-correlation rates are plotted against different regions of a membrane-bound protein cytb$_5$. Error bars correspond to the standard deviation. The mean values of transverse cross-correlation rates for helix, sheet, turn, and loop-region (termini along with linker-region) are 16.08, 15.05, 14.54, and 6.83 s^{-1} with standard deviations of 1.54, 1.43, 2.19, and 2.67 s^{-1}, respectively.

backbone of α-helices and β-sheets wherein the residues experience direct and indirect H-bonding interactions. The large fluctuations of transverse cross-correlation rates in turns and loop-regions are attributed to their more flexible nature, especially in the N-terminus, C-terminus, and the linker region as compared to the residues in α-helices and β-sheets. However, the variation of cross-correlation rates in the individual turns in the structured regions of the cytb$_5$'s soluble domain is slightly less pronounced, indicating less flexibility as compared to the residues in the termini and the linker-region of the protein.

Determination of Backbone Amide-^{15}N CSA Using Transverse Cross-Correlation Rates. The measured backbone amide-^{15}N transverse cross-correlation rates (η_{xy}) were used to determine the span of ^{15}N CSA ($\sigma_{\parallel}-\sigma_{\perp}$) values for membrane-bound cytb$_5$. On the basis of an approach described by Fushman et al., $\eta_{xy}/R_2 = 2dc(P_2(\cos\beta))/(d^2 + c^2)$ was used in our calculation by assuming axially symmetric CSA tensors;[28,29,56] where $d = -\mu_0\gamma_N\gamma_H\hbar/4\pi r^3_{N-H}$ is the dipolar coupling constant, r_{N-H} is the ^{15}N−^{1}H bond length, γ_i is the gyromagnetic ratio of a nucleus i, μ_o is the permeability constant, and $\hbar$ is Plank's constant (h) divided by 2π. The parameter $c = -\omega_N(\sigma_{\parallel}-\sigma_{\perp})/3$ is the CSA constant, where ω_N is the ^{15}N Larmor frequency. $P_2(\cos\beta)$ is the Legendre polynomial, with β representing the angle between the N−H dipolar vector and the least shielded component of the ^{15}N CSA tensor described in principal axis system, and R_2 represents the average transverse relaxation rate. The corresponding backbone amide-^{15}N CSA ($\sigma_{\parallel}-\sigma_{\perp}$) tensors for cytb$_5$ are plotted as a function of the residue number in Figure 6 and are also listed in Table S2 (see the Supporting Information). The calculation of ^{15}N CSA ($\sigma_{\parallel}-\sigma_{\perp}$) tensors for backbone amide residues of cytb$_5$ was performed by assuming effective internuclear distance r_{N-H} =1.023 Å and an angle β = 18°. The ^{15}N CSAs (refer to Table S2 in the Supporting Information) are smaller for residues in the termini and the linker regions as compared to that of the residues in the structured regions of the protein. However, it is important to note that the experimentally determined CSA values for these residues could be inaccurate as they undergo a fast motion in the NMR time scale (ps−ns rotational correlation time) as determined from heteronuclear nuclear Overhauser enhancement along with T_1 and T_2-measurements; the experimentally measured R_2 values are reported in Table S3 of the Supporting

dx.doi.org/10.1021/jp3049229 | J. Phys. Chem. B 2012, 116, 7181−7189

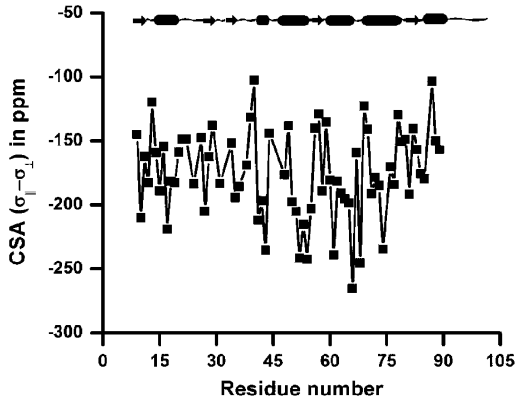

Figure 6. Variation of the backbone amide-^{15}N CSA along the polypeptide chain of the membrane-bound cytb$_5$. The backbone amide-^{15}N CSA for amino acid residues of cytb$_5$ is plotted against the residue number. The ^{15}N CSA values ($\sigma_{\parallel}-\sigma_{\perp}$) were determined by taking an effective internuclear distance between amide nitrogen and proton (r_{N-H}) as 1.023 Å and a constant value for the angle (β = 18°) between N−H bond vector and the CSA tensor described in the principal axis system. CSA values for residues in the N- and C-termini and in the linker-region are not included, as these residues undergo a fast (ns−ps time scale) motion, and the solution NMR approach used in this study may not be suitable for accurately determining their CSA values.

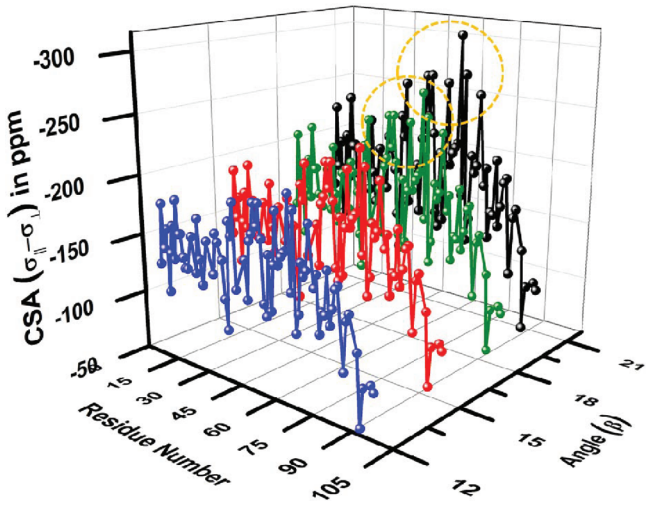

Figure 7. A 3D-plot showing the variation of backbone amide-^{15}N CSA values on angle β. The 3D-plot of ^{15}N CSA values were obtained for β angles of 12° (blue), 15° (red), 18° (green), and 20° (black) against the residue number of cytb$_5$. Circled residues show a larger change in the CSA when changing the angle from 18 to 20°.

Information. Due to such fast motion, CSA tensors can be time-dependent for these residues and therefore the solution NMR method used in this study may not be accurate.[30,45] As a consequence, we have not included these residues in our further analysis of data; in fact, Figure 6 does not include the CSA values for residues in the N- and C-termini and the linker-region.

Dependence of ^{15}N CSA Values on the Angle β. Previous solid-state NMR and quantum chemical calculation studies on peptides have reported that the angle β[2,48,75] in principle could vary from ∼12 to ∼25°. However, for most of the residues, this value was found to lie between 17.5° and 22.5°. In our study, for β = 20°, the mean value of ^{15}N CSA span ($\sigma_{\parallel}-\sigma_{\perp}$) was calculated to be −184.4 ppm, not including the outliers in the termini and the linker regions. This value is slightly more than the commonly used value of −170.0 ppm in the ^{15}N-relaxation studies.

To understand the observed higher average value of ^{15}N CSA for β = 20°, we have compared the change in the CSA for four different angles (12, 15, 18, and 20°) as a function of residue number in membrane-bound cytb$_5$, as shown in Figure 7 (refer to Table S2 in the Supporting Information for ^{15}N CSA values). It is clear from Figure 7 that with the increase in the angle β, i.e., going from 12° to 20°, there is a uniform change of 1−12 ppm in the ^{15}N CSA values for nearly all the residues except the circled ones. For the residues circled in Figure 7, the change in the CSA value is larger as compared to other residues (15−41 ppm versus 1−12 ppm) while increasing the angle from 18° to 20°. This observation is quite obvious from the following inequalities: $\eta_{xy}/R_2 \leq P_2(\cos\beta)$, $\eta_{xy}/R_2 \leq 2dc/(d^2 + c^2)$ and $\eta_{xy}/R_2 \leq 1$, which are required to be simultaneously followed for the experimentally derived CSA.[29] The first inequality determines the upper limit of angle β, while the second determines both the lower and the upper limits of CSA. With the increase in the angle β from 12° to 20°, the value of $P_2(\cos\beta)$ decreases, and, as the difference $\eta_{xy}/R_2 - P_2(\cos\beta)$ becomes narrower (refer to Table S3 in the Supporting Information for (η_{xy}/R_2) values), even a small variation in the angle causes a larger change in the CSA. For illustrative purposes we have taken a case of residue V66 as an example. The calculated backbone amide-^{15}N CSA for V66 at angles 12, 14, 16, 18 and 20° are −215.5, −226.8, −242.4, −265.4, and −306.7 ppm, respectively. The difference in ^{15}N CSA for every 2° increase in angles is 11.3, 15.6, 23.0, and 41.3 ppm, respectively. The value of η_{xy}/R_2 for V66 is 0.81 (corresponding to an upper limit of angle 20.9°), while the values of $P_2(\cos\beta)$ for above listed angles are 0.94, 0.91, 0.89, 0.86, and 0.83. At a constant angle of 20° which is very close to the upper limit of the angle for V66, the difference $(\eta_{xy}/R_2) - P_2(\cos\beta)$ is minimal, leading to an abrupt change in CSA (41.3 ppm) when the angle is changed from 18° to 20°. As a result, we have carried out our calculations at a constant angle (β) of 18° since the variation of ^{15}N CSA is almost uniform for all the residues of a membrane-bound cytb$_5$. The average value of backbone amide-^{15}N CSA for cytb$_5$ (excluding the outliers in the termini and the linker-region) at a constant angle of 18° is found to be −171.7 ppm.

Since ^{15}N CSA values depend on the effective N−H bond length, r_{N-H}, and the angle, β, the choice of r_{N-H} = 1.023 Å and β = 18° for all residues in the protein may not be correct. For example, residues in the unstructured regions can have a different N−H bond length, and Gly residues can have larger β angle based on previous solid-state NMR study.[76] In addition, internal motions can alter the N−H bond length by 10−15% based on the motionally averaged N−H dipolar couplings measured from solid-state NMR studies.[75−78] Even a small deviation of the order of 10^{-2} in the N−H bond length or 1° increase in the β angle could alter the calculated CSA values. To substantiate this aspect, we have calculated the difference in CSA values obtained for r_{N-H} of 1.023 Å and 1.04 Å. The CSA values decrease by a factor of $(1.023/1.04)^3$ = 0.952 with an increase in the N−H bond length with a variation ranging between 5 and 13 ppm (refer to Figure S2 in the Supporting Information). Also as shown in Table S2 of the Supporting Information, even 1° increase in the β angle (going from 17° to 18°) could increase the CSA by 13 ppm.

dx.doi.org/10.1021/jp3049229 | J. Phys. Chem. B 2012, 116, 7181−7189

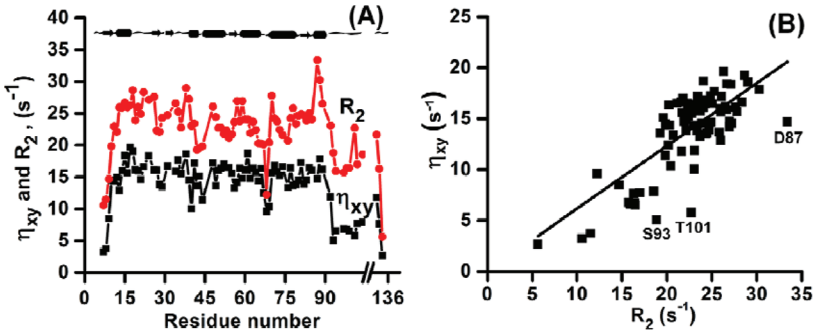

Figure 8. A comparison of the backbone amide-^{15}N transverse cross-correlation rate with the transverse relaxation rate and their linear correlation. Panel A of the plot represents a comparison between the derived backbone amide-^{15}N CSA-dipolar cross-correlation rate (η_{xy}) and the transverse relaxation rate (R_2), while panel B represents a linear correlation with a slope = 0.61 ± 0.01 between these parameters.

Effect of the Paramagnetic Fe(III) on the Backbone Amide-^{15}N CSA of cytb$_5$. On the basis of the observed ^{15}N CSA values, an investigation of the protein dynamics across different structural elements was carried out. For a bond length r_{N-H} = 1.023 Å and the angle β = 18°, the mean value for ^{15}N CSA was found to be larger in the helical region (−187.9 ppm) than in the sheet (−166.0 ppm) and the turn regions (−161.1 ppm), excluding the outliers in the termini and the linker-region. The observed trend is similar to earlier reports on water-soluble proteins,[11,63,77,79] thus validating the ^{15}N CSA dependence on the backbone torsion angles and H-bonding interactions. However, in our case, the observed mean value of ^{15}N CSA for the helical region (−187.9 ppm) of the protein is on the higher side as compared to the average value (−171.7 ppm) for the protein. This observation can be further analyzed on the basis of the interaction of few backbone amide NH nuclei with the low-spin (S = 1/2) paramagnetic center (Fe(III)) of the heme unit of cytb$_5$ that can enhance the ^{15}N-transverse relaxation rates. An increase in the relaxation rate of backbone nuclei (amide protons and nitrogens) in a paramagnetic cytb$_5$, in comparison to the diamagnetic cytb$_5$, is reported elsewhere.[94] The observed paramagnetic effect is reported to be stronger for residues in close proximity to the heme unit, with the largest paramagnetic relaxation enhancement found to be ∼15%. It may also be possible that this interaction causes an additional contribution in the form of cross-correlation between CSA and dipolar shielding anisotropy (DSA)[80,81] due to the thermally averaged electronic spin (Curie spin)[82,83] of the paramagnetic Fe(III). For a paramagnetic center, this contribution cannot be ignored for smaller distances from the Fe(III) at higher magnetic field strengths. The CSA × DSA cross-correlation rate depends on the relative orientation of the principal components of CSA and DSA tensors and is inversely proportional to the cube of the distance between the nuclear and the electronic spin. In cytb$_5$, the residues L41, E42, E43, E48, E49, V50, L51, R52, E53, Q54, T60, E61, N62, F63, E64, D65, V66, D71, A72, R73, E74, L75, S76, K77, F79 (all from helical region), L30, Y35 (from beta-sheet), H31, L37, T38, F40, H44, A59, G67, H68, and S69 (all from turn) are in close proximity (<12.5 Å) to the paramagnetic center Fe(III) of the heme unit (refer to Figure S1 in the Supporting Information). Most of these residues such as H31, Y35, L41, E42, E43, E48, V50, L51, R52, E53, Q54, T60, E61, N62, F63, E64, D65, V66, G67, H68, D71, A72, R73, E74, and S76 (refer to Table S2 in Supporting Information for values of ^{15}N CSA) show relatively higher span of ^{15}N CSA, which is possibly because of the effective shielding due to CSA × DSA cross-correlation effect. Also, it is important to note that most of the residues interacting with the paramagnetic center exhibiting a larger span of ^{15}N CSA are from the helical region; hence the observed mean value is higher for helical region residues as compared to reported values. The ^{15}N CSA for backbone amide residues (D87, D88, and R89) in the last helix along the polypeptide chain are small when compared to most of the other helical residues in the protein. These residues are situated at a larger distance (>25.0 Å) from the paramagnetic center, and as a result their interaction with paramagnetic center is less pronounced, leading to a smaller ^{15}N CSA. This also validates the dependence of the ^{15}N CSA for structured regions on the distance from the paramagnetic center. Residues such as T38, F40, H44, A59, and S69 show relatively lower values of ^{15}N CSA, even if they are in close proximity with the paramagnetic center. These residues are in the turn regions of the protein sequence, and their flexibility may reduce the observed ^{15}N CSA values. Spectral overlap for the residues L30, L37 and L75, debarred them from the ^{15}N CSA analysis.

Site-Specific Variation of the Backbone Amide-^{15}N CSA in cytb$_5$. The calculated ^{15}N-transverse cross-correlation rates (η_{xy}) for various residues of cytb$_5$ have a linear correlation (slope = 0.61 ± 0.01) with transverse relaxation rate (R_2) as shown in Figure 8. This is in accordance with the theoretical calculation by Fushman and Cowburn.[28] The uniform spread of data points around the average-slope line shows site-specific variations in the ^{15}N CSA values for cytb$_5$. The outliers in the plot are mostly from the linker region (e.g., S93 and T101). An exception is the D87 residue located in the helical region but next to the Pro86 residue that breaks the secondary structure in the sequence, which could reduce the CSA as observed in our study.

To further validate the site-specific variation of CSA, a bar graph is plotted in Figure 9 that shows a Gaussian spread of η_{xy}/R_2 values for various residues in cytb$_5$. The spread starts from 0.4 (excluding the residues in N- and C-termini and in the linker-region) and ends at 0.81 with a mean value of 0.68. Past studies have shown the site-specific variation of ^{15}N CSA both in solution as well as in the solid-state. ^{15}N CSA determined for short peptides and proteins from solid-state NMR studies show a narrow range of variation as compared to solution NMR studies (refer to Tables S4, S5, and S6 in the Supporting Information).[11,16,76] On the basis of the amide-^{15}N CSA values reported in a recent review article,[16] the ^{15}N CSA values in solid-state varies from 139.8 to 168.8 ppm. The difference between the values reported from solid-state and solution NMR studies is mainly because the solution NMR approach applies a

dx.doi.org/10.1021/jp3049229 | J. Phys. Chem. B 2012, 116, 7181−7189

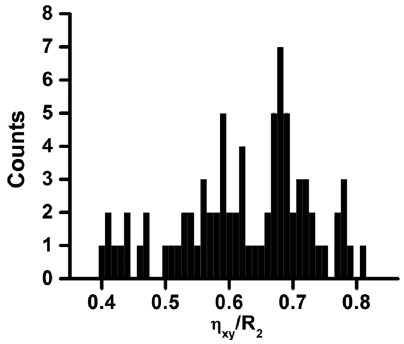

Figure 9. Distribution of η_{xy}/R_2 in cytb$_5$. The plot represents a Gaussian distribution of the ratio of transverse cross-correlation (η_{xy}) and transverse relaxation rates (R_2). The mean value of the distribution is 0.68.

correction for the effects of small amplitude internal motion, while solid-state NMR utilizes the motionally averaged CSA and N−H dipolar couplings.[32] This is also confirmed by a recent theoretical study, using automated fragmentation quantum mechanics/molecular mechanics (AF-QM/MM) on crystal structures of GB1 and GB3 proteins, that reported CSA values that are in agreement with solid-state NMR values.[54] The site-specific CSAs determined from solution NMR studies for ubiquitin, ribonuclease H, and GB3 were reported to be −125 to −216 ppm,[29] −129 to −213 ppm,[30] and −111 to −241 ppm,[61] respectively. In the present study, the backbone amide-^{15}N CSA exhibits even a larger range of CSA: −123 ppm to −245 ppm (excluding the outliers: a turn residue F40, D87 attached to Pro86, and residues in termini and linker regions) with an exception of 265 ppm for V66 residue that is very close to Fe(III). While most values reported in this study are in good agreement with previous solution NMR studies, the higher CSA values for certain residues reported in this study may be attributed to the effect of the interaction of backbone nuclei (^{15}N and ^{1}H) with the paramagnetic center of the heme unit in addition to the uncertainty in the internuclear distance (r_{N-H}) and angle β as discussed above. Nevertheless, the average amide-^{15}N CSA value of −171.7 ppm determined for cytb$_5$ (excluding the outliers in the termini and the linker regions) is found to be consistent with earlier reports from solid-state NMR studies on peptides using a ^{15}N-dipolar coupled powder pattern,[1,2,75,76,84−90] ^{15}N NMR of a single crystal,[91,92] static[93−96] spectra, and solution NMR studies on water-soluble proteins[30,61,63,97−99] (refer to Tables S4, S5 and S6 in the Supporting Information).

CONCLUSIONS

In summary, we have measured ^{15}N CSA/dipolar transverse cross-correlation rates using ^{1}H-coupled ^{15}N−^{1}H HSQC-type IPAP spectra to determine ^{15}N CSA tensors for backbone amide residues in a full-length membrane-bound protein cytb$_5$ incorporated in DPC micelles to understand the overall dynamics of the protein. A narrow span of ^{15}N transverse correlation rates is observed in the structured regions suggesting a uniform characteristic of ^{15}N cross-correlated relaxation, while the larger variation observed in the termini and linker-region suggests a highly dynamic nature. The mean value of backbone amide-^{15}N CSA of cytb$_5$ excluding the outliers in the termini and linker-region is found to be −171.7 ppm for an NH bond length of 1.023 Å and at β = 18°, the angle the least shielded component of the tensor makes with the N−H bond. The average values of ^{15}N CSA for residues in the helical, sheet, and turn regions are −187.9, −166.0, and −161.1 ppm, respectively. Larger CSA values observed for helical residues of the protein as compared to previous solution NMR values is possibly due to the enhanced CSA/DSA cross-correlation rate resulting from the interaction of the amide nitrogens and protons with the paramagnetic center Fe(III) of the heme unit. Therefore, it is worth characterizing the paramagnetic effect on the experimentally measured CSA values in such paramagnetic proteins. We believe that this study will be a step forward to better understand the structure, dynamics, and orientation of membrane proteins based on well-characterized backbone amide-^{15}N CSA values using NMR spectroscopy.

ASSOCIATED CONTENT

Supporting Information

Tables for measured backbone amide-^{15}N transverse cross-correlation rates (η_{xy}); calculated backbone amide-^{15}N CSA; ratio of transverse cross-correlation rates (η_{xy}) and transverse relaxation rates (R_2); ^{15}N CSA values determined from past studies. Figures showing residues of cytb$_5$ that are located within 12.5 Å distance from paramagnetic center Fe(III) of the heme unit and difference in ^{15}N CSA calculated for two different values of internuclear distance. This material is available free of charge via the Internet at http://pubs.acs.org.

AUTHOR INFORMATION

Corresponding Author

*E-mail: ramamoor@umich.edu.

Notes

The authors declare no competing financial interest.

ACKNOWLEDGMENTS

We would like to thank Professor David Fushman, University of Maryland, for providing us with the NMR pulse program. This research is supported by funds from the NIH (GM084018 and GM095640 to A.R.).

REFERENCES

(1) Hartzell, C. J.; Whitfield, M.; Oas, T. G.; Drobny, G. P. *J. Am. Chem. Soc.* **1987**, *109*, 5966.
(2) Oas, T. G.; Hartzell, C. J.; Dahlquist, F. W.; Drobny, G. P. *J. Am. Chem. Soc.* **1987**, *109*, 5962.
(3) Oas, T. G.; Hartzell, C. J.; McMahon, T. J.; Drobny, G. P.; Dahlquist, F. W. *J. Am. Chem. Soc.* **1987**, *109*, 5956.
(4) Linder, M.; Höhener, A.; Ernst, R. R. *J. Chem. Phys.* **1980**, *73*, 4959.
(5) Hester, R. K.; Ackerman, J. L.; Neff, B. L.; Waugh, J. S. *Phys. Rev. Lett.* **1976**, *36*, 1081.
(6) Wu, C. H.; Ramamoorthy, A.; Opella, S. J. *J. Magn. Reson. A* **1994**, *109*, 270.
(7) Maricq, M. M.; Waugh, J. S. *J. Chem. Phys.* **1979**, *70*, 3300.
(8) Ramamoorthy, A.; Opella, S. J. *Solid State Nucl. Magn. Reson.* **1995**, *4*, 387.
(9) Hertzfeld, J.; Berger, A. E. *J. Chem. Phys.* **1980**, *73*, 6021.
(10) Wylie, B. J.; Franks, W. T.; Graesser, D. T.; Reinstra, C. M. *J. Am. Chem. Soc.* **2005**, *127*, 11946.
(11) Wylie, B. J.; Sperling, L. J.; Frericks, H. L.; Shah, G. J.; Franks, W. T.; Reinstra, C. M. *J. Am. Chem. Soc.* **2007**, *129*, 5318.
(12) Tycko, R.; Dabbagh, G.; Mirau, P. A. *J. Magn. Reson.* **1989**, *85*, 265.
(13) Chan, J. C. C.; Tycko, R. *J. Chem. Phys.* **2003**, *118*, 8378.
(14) Yao, X.; Hong, M. *J. Am. Chem. Soc.* **2002**, *124*, 2730.

(15) Shekar, S. C.; Ramamoorthy, A.; Wittebort, R. J. *J. Magn. Reson.* **2002**, *155*, 257.
(16) Saitô, H.; Ando, I.; Ramamoorthy, A. *Prog. Nucl. Magn. Reson. Spectrosc.* **2010**, *57*, 181.
(17) Naito, A.; Ganapathy, S.; Akasaka, K.; McDowell, C. A. *J. Chem. Phys.* **1981**, *74*, 3190.
(18) Facelli, J. C. Modeling NMR Chemical Shifts. In *Modern Magnetic Resonance*, Webb, G. A., Ed.; Springer: Dordrecht, The Netherlands, 2006; Vol. *1*, p 53.
(19) Oldfield, E. *Annu. Rev. Phys. Chem.* **2002**, *53*, 349.
(20) Fukui, H. *Prog. Nucl. Magn. Reson. Spectrosc.* **1997**, *31*, 317.
(21) de Dios, A. C.; Oldfield, E. *J. Am. Chem. Soc.* **1994**, *116*, 11485.
(22) de Dios, A. C. *Prog. Nucl. Magn. Reson. Spectrosc.* **1996**, *29*, 229.
(23) Sitkoff, D.; Case, D. A. *Prog. Nucl. Magn. Reson. Spectrosc.* **1998**, *32*, 165.
(24) Ando, I.; Kuroki, S.; Kurosu, H.; Yamanobe, T. *Prog. Nucl. Magn. Reson. Spectrosc.* **2001**, *39*, 79.
(25) Karadakov, P. Ab Initio Calculation of NMR Shielding Constants. In *Modern Magnetic Resonance*; Webb, G. A., Ed.; Springer: Dordrecht, The Netherlands, 2006; Vol. *1*, p 59.
(26) Loth, K.; Pelupessy, P.; Bodenhausen, G. *J. Am. Chem. Soc.* **2005**, *127*, 6062.
(27) Goldman, M. *J. Magn. Reson.* **1984**, 60.
(28) Fushman, D.; Cowburn, D. *J. Am. Chem. Soc.* **1998**, *120*, 7109.
(29) Fushman, D.; Tjandra, N.; Cowburn, D. *J. Am. Chem. Soc.* **1998**, *120*, 10947.
(30) Kroenke, C. D.; Rance, M.; Palmer, A. G., III. *J. Am. Chem. Soc.* **1999**, *121*, 10119.
(31) Lienin, S. F.; Bremi, T.; Brustscher, B.; Brüchweiler, R.; Ernst, R. R. *J. Am. Chem. Soc.* **1998**, *120*, 9870.
(32) Tjandra, N.; Szabo, A.; Bax, A. *J. Am. Chem. Soc.* **1996**, *118*, 6986.
(33) Früh, D.; Chiarparin, E.; Pelupessy, P.; Bodenhausen, G. *J. Am. Chem. Soc.* **2002**, *124*, 4050.
(34) Walker, O.; Mutzenhardt, P.; Tekely, P.; Canet, D. *J. Am. Chem. Soc.* **2002**, *124*, 865.
(35) Markwick, P. R. L.; Sattler, M. *J. Am. Chem. Soc.* **2004**, *126*, 11424.
(36) Wylie, B. J.; D., S. C.; Oldfield, E.; Reinstra, C. M. *J. Am. Chem. Soc.* **2009**, *131*, 985.
(37) Havlin, R. H.; Laws, D. D.; Bitter, H.-M. L.; Sanders, L. K.; Sun, H.; Grimley, J. S.; Wemmer, D. E.; Pines, A.; Oldfield, E. *J. Am. Chem. Soc.* **2001**, *123*, 10362.
(38) Birn, J.; Poon, A.; Mao, Y.; Ramamoorthy, A. *J. Am. Chem. Soc.* **2004**, *126*, 8529.
(39) Tessari, M.; Mulder, F. A. A.; Boelens, R.; W., V. G. *J. Magn. Reson.* **1997**, *127*, 128.
(40) Tugarinov, V.; Scheurer, C.; Brüschweiler, R.; Kay, L. E. *J. Biomol. NMR* **2004**, *30*, 397.
(41) Ramamoorthy, A.; Wu, C. H.; Opella, S. J. *J. Am. Chem. Soc.* **1997**, *119*, 10479.
(42) Wei, Y.; de Dios, A. C.; McDermott, A. E. *J. Am. Chem. Soc.* **1999**, *121*, 10389.
(43) de Dios, A. C.; Pearson, J. G.; Oldfield, E. *Science* **1993**, *260*, 1491.
(44) Ferraro, M. B.; Repetto, V.; Facelli, J. C. *Solid State Nucl. Magn. Reson.* **1998**, *10*, 185.
(45) Scheurer, C.; Skrynnikov, R.; Lienin, S. F.; Straus, S. K.; Brüschweiler, R.; Ernst, R. *J. Am. Chem. Soc.* **1999**, *121*, 4242.
(46) Hu, J. Z.; Facelli, J. C.; Alderman, D. W.; Pugmire, R. J.; Grant, D. M. *J. Am. Chem. Soc.* **1998**, *120*, 9863.
(47) Walling, A. E.; Pargas, R. E.; de Dios, A. C. *J. Phys. Chem. A* **1997**, *101*, 7299.
(48) Brender, J. R.; Taylor, D. M.; Ramamoorthy, A. *J. Am. Chem. Soc.* **2001**, *123*, 914.
(49) Cai, L.; F., D.; Kosov, D. S. *J. Biomol. NMR* **2008**, *41*, 77.
(50) Cai, L.; Fushman, D.; Kosov, D. S. *J. Biomol. NMR* **2009**, *45*, 245.
(51) Poon, A.; Birn, J.; Ramamoorthy, A. *J. Phys. Chem. B* **2004**, *108*, 16577.
(52) Le, H.; Oldfield, E. *J. Phys. Chem.* **1996**, *100*, 16423.
(53) Cai, L.; Kosov, D. S.; Fushman, D. *J. Biomol. NMR* **2011**, *50*, 19.
(54) Tang, S.; Case, D. A. *J. Biomol. NMR* **2011**, *51*, 303.
(55) Strohmeier, M.; Grant, D. M. *J. Am. Chem. Soc.* **2004**, *126*, 966.
(56) Hall, J. B.; Fushman, D. *Magn. Reson. Chem.* **2003**, *41*, 837.
(57) Hall, J. B.; Dayie, K. T.; Fushman, D. *J. Biomol. NMR* **2003**, *26*, 181.
(58) Fushman, D.; Tjandra, N.; Cowburn, D. *J. Am. Chem. Soc.* **1999**, *121*, 8577.
(59) Canet, D.; Barthe, P.; Mutzenhardt, P.; Roumestand, C. *J. Am. Chem. Soc.* **2001**, *123*, 4567.
(60) Cisnetti, F.; Loth, K.; Pelupessy, P.; Bodenhausen, G. *ChemPhysChem* **2004**, *5*, 807.
(61) Hall, J. B.; Fushman, D. *J. Am. Chem. Soc.* **2006**, *128*, 7855.
(62) Damberg, P.; Jarvet, J.; Gräslund, A. *J. Am. Chem. Soc.* **2005**, *127*, 1995.
(63) Yao, L.; Grishaev, A.; Cornilescu, G.; Bax, A. *J. Am. Chem. Soc.* **2010**, *132*, 4295.
(64) Im, S.-C.; Waskell, L. *Arch. Biochem. Biophys.* **2011**, *507*, 144.
(65) Schenkman, J. B.; Jansson, I. *Pharmacol. Ther.* **2003**, *97*, 139.
(66) Ahuja, S.; Vivekanandan, S.; Popovych, N.; Le Clair, S. V.; Soong, R.; Yamamoto, K.; Xu, J.; Nanga, R. P. R.; Im, S.-C.; Waskell, L.; Ramamoorthy, A. NMR Structural Studies of a Membrane-Associated (>70 kDa) Complex between Cytochrome P450 and b5. Poster-204 in The 52nd Experimental Nuclear Magnetic Resonance Conference, Asilomar Conference Grounds, Pacific Grove, CA, April 10−15, 2011.
(67) Mulrooney, S. B.; Waskell, L. *Protein Expression Purif.* **2000**, *19*, 173.
(68) Delaglio, F.; Grzesiek, S.; Vuister, G. W.; Zhu, G.; Pfeifer, J.; Bax, A. *J. Biomol. NMR* **1995**, *6*, 277.
(69) Kneller, D. G.; Kuntz, I. D. *J. Cell. Biochem.* **1993**, 254.
(70) K., P.; G., W.; K., W. *J. Biomol. NMR* **1998**, *12*, 345.
(71) Dvinskikh, S. V.; Yamamoto, K.; Ramamoorthy, A. *J. Chem. Phys.* **2006**, *125*, 034507.
(72) Caravatti, P.; Braunschweiler, L.; Ernst, R. R. *Chem. Phys. Lett.* **1983**, *100*, 305.
(73) Ottiger, M.; Delaglio, F.; Bax, A. *J. Magn. Reson.* **1998**, *131*, 373.
(74) Tjandra, N.; Feller, S. E.; Pastor, R. W.; Bax, A. *J. Am. Chem. Soc.* **1995**, *117*, 12562.
(75) Wu, C. H.; Ramamoorthy, A.; Gierasch, L. M.; Opella, S. J. *J. Am. Chem. Soc.* **1995**, *117*, 6148.
(76) Lee, D. K.; Wittebort, R. J.; Ramamoorthy, A. *J. Am. Chem. Soc.* **1998**, *120*, 8868.
(77) Cornilescu, G.; Bax, A. *J. Am. Chem. Soc.* **2000**, *122*, 10143.
(78) Roberts, J. E.; Harbison, G. S.; Munowitz, M. G.; Herzfeld, J.; Griffin, R. G. *J. Am. Chem. Soc.* **1987**, *109*, 4163.
(79) Wylie, B. J.; Reinstra, C. M. *J. Chem. Phys.* **2008**, *128*, 052207.
(80) Pintacuda, G.; Kaikkonen, A.; Otting, G. *J. Magn. Reson.* **2004**, *171*, 233.
(81) Otting, G. *Annu. Rev. Biophys.* **2010**, *39*, 387.
(82) Gueron, M. *J. Magn. Reson.* **1975**, *19*, 58.
(83) Vega, A. J.; Fiat, D. *Mol. Phys.* **1976**, *31*, 347.
(84) Mai, W.; Hu, W.; Wang, C.; Cross, T. A. *Protein Sci.* **1993**, *2*, 532.
(85) Fukutani, A.; Naito, A.; Tuzi, S.; Saitô, H. *J. Mol. Struct.* **2002**, *602*, 491.
(86) Hiyama, Y.; Niu, C. H.; Silverton, J. V.; Bavoso, A.; Torchia, D. A. *J. Am. Chem. Soc.* **1988**, *110*, 2378.
(87) Lee, D. K.; Wei, Y.; Ramamoorthy, A. *J. Phys. Chem. B* **2001**, *105*, 4752.
(88) Chekmenev, E. Y.; Zhang, Q.; Waddell, K. W.; Mashuta, M. S.; Wittebort, R. J. *J. Am. Chem. Soc.* **2003**, *126*, 379.
(89) Wei, Y.; Lee, D.-K.; McDermott, A. E.; Ramamoorthy, A. *J. Magn. Reson.* **2002**, *158*, 23.
(90) Lee, D. K.; Santos, J. S.; Ramamoorthy, A. *Chem. Phys. Lett.* **1999**, *309*, 209.

(91) Waddell, K. W.; Chekmenev, E. Y.; Wittebort, R. J. *J. Am. Chem. Soc.* **2005**, *127*, 9030.
(92) Harbison, G. S.; Jelinski, L. W.; Stark, R. E.; Torchia, D. A.; Herzfeld, J.; Griffin, R. G. *J. Magn. Reson.* **1984**, *60*, 79.
(93) Shoji, A.; Ozaki, T.; Fujito, T.; Deguchi, K.; Ando, S.; Ando, I. *J. Am. Chem. Soc.* **1990**, *112*, 4693.
(94) Shoji, A.; Ozaki, T.; Fujito, T.; Deguchi, K.; Ando, S.; Ando, I. *Macromolecules* **1989**, *22*, 2860.
(95) Ashikawa, M.; Shoji, A.; Ozaki, T.; Ando, I. *Macromolecules* **1999**, *32*, 2288.
(96) Shoji, A.; Ozaki, T.; Fujito, T.; Deguchi, K.; Ando, I.; Magoshi, J. *J. Mol. Struct.* **1998**, *441*, 251.
(97) Boyd, J.; Redfield, C. *J. Am. Chem. Soc.* **1999**, *121*, 7441.
(98) Kurita, J.; Shimahara, H.; Utsunomiya-Tate, N.; Tate, S. *J. Magn. Reson.* **2003**, *163*, 163.
(99) Tjandra, N.; Wingfield, P.; Stahl, S.; Bax, A. *J. Biomol. NMR* **1996**, *8*, 273.